arXiv:cond-mat/0607198v2 [cond-mat.supr-con] 30 Aug 2006

Insights from ARPES for an undoped, four-layered, two-gap high-T_c superconductor

Wenhui Xie,[1] O. Jepsen,[1] O. K. Andersen,[1] Yulin Chen,[2] and Z.-X. Shen[2]
[1] *Max-Planck Institut für Festkörperforschung, Heisenbergstr. 1, D-70569 Stuttgart, Germany*
[2] *Stanford Synchrotron Radiation Laboratory, Stanford University, Stanford, Ca, USA*

(Dated: February 3, 2008)

An undoped cuprate with apical fluorine and inner (i) and outer (o) CuO_2-layers is a 60 K superconductor whose Fermi surface (FS) has large n and p-doped sheets with the SC gap on the n-sheet twice that on the p-sheet [1]. The Fermi surface is *not* reproduced by the LDA, but the screening must be substantially reduced due to electronic correlations, *and* oxygen in the o-layers must be allowed to dimple outwards. This charges the i-layers by $0.01|e|$, causes an 0.4 eV Madelung-potential difference between the i and o-layers, quenches the i-o hopping, and localizes the n-sheets onto the i-layers, thus protecting their d-wave pairs from being broken by scattering on impurities in the BaF layers. The correlation-reduced screening strengthens the coupling to z-axis phonons.

PACS numbers: 71.18.+y,74.25.Jb,74.72.Jt

Despite 20 years' intensive research, high-temperature superconductivity in the cuprates has not been understood. Much insight has been gained through discoveries of new cuprates and refinements of experimental techniques. An example is the discovery [2] of an undoped 4-layered cuprate with apical fluorine, $Ba_2Ca_3Cu_4O_8F_2$, which is not a Mott insulator, but a 60 K HTSC; the experimental findings about its Fermi surface and SC gap are reported in the preceding Letter [1].

All HTSCs consist of CuO_2-layers separated by apical blocks into which dopants may be inserted. Undoped cuprates (Cu $3d^9$) are antiferromagnetic (AF) Mott insulators. Upon hole-doping beyond $p{\sim}0.05$ per CuO_2, they become HTSCs with pairing symmetry $d_{x^2-y^2}$, and the critical temperature reaches a maximum, $T_{c\,\max}$, when $p{\sim}0.2$. For optimally and over-doped materials the Fermi surfaces (FS) measured by ARPES enclose *large* hole-areas of size $1+p$ (in units of half the Brillouin-zone area), are centered at $(k_x, k_y) = (\pi, \pi)$, and agree surprisingly well with detailed predictions from LDA band-structure calculations [3]. Even the existence of a small sub-band splitting in bi-layered cuprates [4, 5], which is twice the integral for inter-layer hopping, $t_\perp(\mathbf{k}_\parallel) \sim t_\perp(\cos k_x - \cos k_y)^2/4$, and the existence of a k_z-dispersion proportional to $t_\perp(\mathbf{k}_\parallel)\cos\frac{1}{2}k_x \cos\frac{1}{2}k_y \cos\frac{c}{2}k_z$ in body-centered tetragonal materials [6, 7], have recently been confirmed by ARPES [3, 8] and angular magnetoresistance oscillations (AMRO) [9]. Hence, over- and optimally doped cuprates appear to have well-defined quasi-particle bands with mass-renormalizations 2-4, not only in the direction of the layers, but also in the perpendicular direction [3, 10, 11]. In the superconducting state, the magnitude of the gap is approximately $5.5k_BT_c$. For under-doped materials, a pseudogap opens up when $T < T^*$. The remaining Fermi arcs [3, 12], when mirrored around the AF zone boundary, enclose *small* hole-areas of size p, are centered at $\left(\frac{\pi}{2}, \frac{\pi}{2}\right)$, and are roughly reproduced by LDA+U calculations with $U_{dd}{\sim}6$ eV and AF long-range order, or similar Hartree-Fock (HF) solutions for 3-band models [5, 13]. Upon doping with electrons beyond a certain level, a metallic AF (AFM) phase develops and, subsequently, a superconducting phase with the electrons occupying *small,* $(\pi, 0)$-centered FS areas of size n. For higher n-doping [3, 14], antiferromagnetism disappears and the FS again becomes (π, π)-centered and large, of size $1-n$. Optimal n-doping occurs for $n{\sim}0.2$, and known values of $T_{c\ \max}$ are much smaller ($\lesssim 40$ K) than for optimal p-doping ($\lesssim 140$ K), and so are the gaps. So far it has not been possible to p- and n-dope the same compound.

In Fig. 1, we show the FS of undoped $Ba_2Ca_3Cu_4O_8F_2$. ARPES resolves the two sheets shown in grey [1]. Both are (π, π)-centered and *large,* their areas being $1 \pm p$ with $p{\sim}0.2$. We shall refer to the larger one as the hole-doped or p-sheet and to the smaller one as the electron-doped or n-sheet. $Ba_2Ca_3Cu_4O_8F_2$ thus appears to be the first *self*-doped HTSC having n- and p-doping in one and the same crystal. All other known undoped cuprates, single- as well as multi-layered, are insulating, and when hole-doped, the observed FS-area splittings [8] are proportional to $t_\perp(\mathbf{k}_\parallel)$ and almost an order of magnitude smaller than the ± 0.2 found in $Ba_2Ca_3Cu_4O_8F_2$. The question we shall try to answer in this letter is: How and why does this compound manage to dope itself?

There are no FS measurements for multi-layered cuprates with *in*equivalent inner (i) and outer (o) layers, with the exception of $Ba_2Ca_3Cu_4O_8F_2$, but *site-selective* NMR studies [15] indicate that i-layers have less holes than o-layers and that superconductivity develops differently with temperature in the different layers. This behaviour is interpreted in terms of electrons localized onto individual layers, each of which follows the generic phase diagram as a function of doping, and which are weakly coupled by proximity effects [16]. Most spectacular are the properties of 5-layered $HgBa_2Ca_4Cu_5O_{12+\delta}$ [17]. Here, the o-layers form an optimally doped HTSC with $T_{c\,\max}$=108 K and the three i-layers are AF *metals* (AFM) with moments of about $0.3\mu_B$. By decreasing the

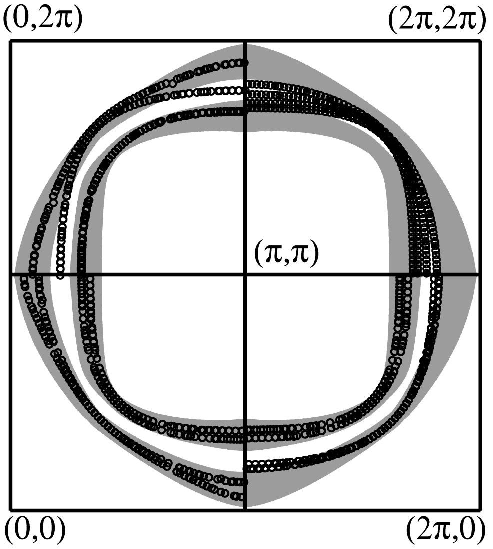

FIG. 1: FS for $Ba_2Ca_3Cu_4O_8F_2$. *Grey:* ARPES [1]. The width reflects the experimental error bar. The smaller (larger) sheet is the $n\,(p)$-sheet. *Open dots:* Calculations. *Top right:* LDA. *Remaining three quarters:* $\langle$LDA+$U\rangle$. *Bottom right:* Flat CuO_2-layers and 2% F-O exchange (q=0.02) treated in the VCA. Indistinguishable from this FS are the ones calculated with no F-O exchange, but with O in the o- or i-layers dimpled outwards by 0.07 Å. See Fig. 3. The $n\,(p)$-sheet resides on the $i\,(o)$-layers. ε_F is adjusted such the FS fits along the nodal line whereby n=0.19 and p=0.12. *Bottom left:* Dimpling as before, but with the vertical Ba and F positions adjusted such as to give the best agreement with the ARPES FS: $z_{\mathrm{Ba}}-z_{\mathrm{Cu}_o}$ is decreased from 2.0 to 1.7Å and $z_{\mathrm{F}}-z_{\mathrm{Cu}_o}$ is decreased from 2.4 to 2.1Å. ε_F is adjusted as before, whereby n=0.18 and p=0.21. *Top left:* As before but with O in the o- (or i-) layers dimpled *inwards* by 0.10 Å. Now, the $n\,(p)$-sheet resides on the $o\,(i)$-layers. $z_{\mathrm{Ba}}-z_{\mathrm{Cu}_o}=1.6$Å and $z_{\mathrm{F}}-z_{\mathrm{Cu}_o}=2.0$Å. ε_F is adjusted as before, whereby n=0.15 and p=0.18. Note that inter-sheet splittings in **k**-space are enhanced near the saddlepoints in the band structure.

hole doping, T_c decreases to 70 K and the o-layers form a *uniformly* mixed HTSC-AFM phase with $0.1\mu_B$ moments while the i-layers form a $0.7\mu_B$-AFM. The layers are flat and the estimated hole-counts for the o- and i-layers differ by as much as 0.2 for the over-doped material.

Seen on the background of these truly exotic properties, the discovery [1] that $Ba_2Ca_3Cu_4O_8F_2$ is the first HTSC with *different SC gaps* on the two sheets, may seem less spectacular. However, it is the gap on the n-sheet which is the largest, actually twice the gap on the p-sheet, and this is opposite to what one would expect from the generic phase diagram. Moreover, two-gap superconductivity has only been observed unambiguously in a few materials of which MgB_2 is the most spectacular. There, the mechanism is conventional [18, 19].

Whereas the FS sheets observed in all other multi-layered HTSCs are hardly split along the nodal direction, $Ba_2Ca_3Cu_4O_8F_2$ exhibits a *large nodal splitting,* $\Delta k_{[110]}$. This is the *third* anomaly of the ARPES data and the key to the self-doping and the two gaps. For comparison with the ARPES FS, we show in the top right-hand quarter of Fig. 1 the LDA FS which is seen to have four FS sheets, split almost exclusively by inter-layer hopping [20]. The four sub-bands are split by approximately $\pm\frac{1}{2}\left(\sqrt{5}\pm 1\right)t_\perp\left(\mathbf{k}_{\shortparallel}\right)$ with $t_\perp\sim$0.2 eV. This is the first case known to us where there is a substantial *discrepancy* between an experimental, large FS and the LDA. The latter fails to reproduce the $\Delta k_{[110]}\,\partial\varepsilon/\partial k_{[110]}=0.4$ eV large *Madelung-potential difference* (on electron scale) between the layers on which respectively the p- and the n-nodal quasi-particles are located. We have taken $\partial\varepsilon/\partial k_{[110]}$ as the bare (LDA) nodal velocity, which is the consistent choice in the present context [21]. In the LDA (GGA), the electron potential averaged over an i-layer is 0.024 eV (0.034 eV) less than that averaged over an o-layer, that is 17 (12) times too small! The discrepancy remains after we optimize the structure using the LDA. Thereby, most notably, the oxygens in the o-layers dimple outwards by $\sim 3°$, about one third the dimple in $YBa_2Cu_3O_7$ [22].

Since the 0.4 eV potential exceeds $\frac{1}{2}\left(\sqrt{5}+1\right)t_\perp$, it effectively *blocks the hopping* between the i- and the o-layers. Therefore, the n-sheets are associated with the i-layers and the p-sheets with the o-layers, or the other way around. The potential difference thus blocks inter-band scattering and protects the i-bands from scattering on the ubiquitous impurities in the apical BaF-blocks. This may be the reason why two SC gaps survive and –in case the p-sheets reside on the o-layers– also the reason why the gap on the p-sheets is the smaller one: it is suppressed by scattering on impurities in the BaF-block.

Let us set this 0.4 eV potential difference in perspective: With the in-plane lattice constant 3.86 Å and the distance between Ca and CuO_2 layers 1.54 Å, Poisson's equation says that the layer-averaged potential is a saw-tooth with kinks of $\sim$20 eV Q_n on the layers. Q_n is the charge per 2D cell. If $Ba_2Ca_3Cu_4O_8F_2$ were purely ionic, the potential would therefore be 0 on the Ca^{2+} layers and 20 eV on the $\left(CuO_2\right)^{2-}$ layers, the *same* on the i- and o-layers because the $CaCuO_2$-*unit is neutral.* Next, we transfer from the BaF layers q_i positive charges to each of the i-layers and q_o positive charges to each of the o-layers. This sets up a difference in Madelung potential between o- and i-layers of $40q_i$ eV, which depends only on q_i, not on q_o.The ARPES value of 0.4 eV (neglecting exchange-correlation contributions) therefore tells us that the i-layers have a net charge of either $0.01\,|e|$, in which case the n-sheets reside on the i-layers, or of $-0.01\,|e|$, in which case the p-sheets are on the i-layers. In the LDA (GGA), the charging is 17 (12) times smaller.

Crystallographically it is possible that q of the two layer-oxygens per cell are exchanged with fluorine, so that the formula is $Ba_2Ca_3(CuO_{2-q}F_q)_4O_{4q}F_{2-4q}$. In fact, LDA calculations with q=0.25, employing not only

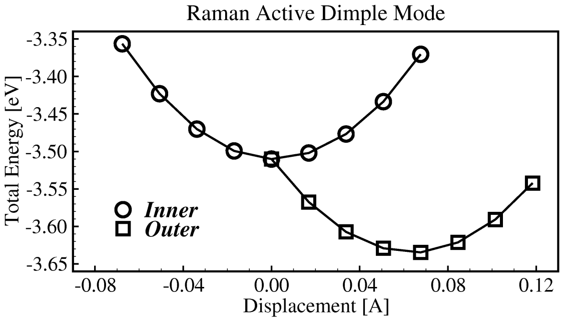

FIG. 2: Total energy as a function of the Raman-active dimpling displacements calculated with LDA+U. See Fig. 3.

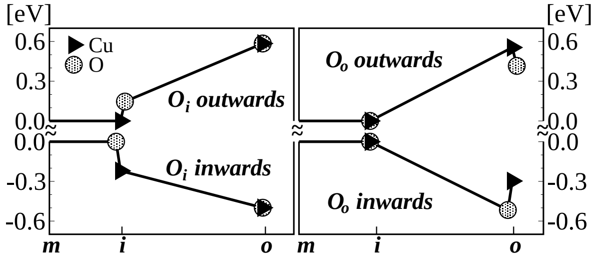

FIG. 3: Layer-averaged potentials calculated with $\langle$LDA+$U\rangle$ for dimplings of ±0.1 Å of the inner (left) and outer (right) layer-oxygens. This potential is the calculated Cu and O core levels, lined up on the flat layer and normalized to zero at the Ca mirror plane. m is the mirror plane.

the virtual-crystal approximation (VCA), but also supercells, *do* reproduce the ARPES FS. However, the position of the apical F $2p_z$ level is 4 eV below that of apical O $2p_z$, and such impurities in the CuO$_2$-layers are very efficient in breaking $d_{x^2-y^2}$-wave pairs: For an allowed T_c-suppression of 10%, we find that q cannot exceed 0.001, which is even smaller than the charging of 0.01 needed to create the observed crystal-field splitting in the absence of screening [23]. This rules out F-O exchange as an explanation for the anomalous ARPES FS.

QMC calculations for a t_{1u}-band Hubbard model for C$_{60}$ have revealed that the RPA describes metallic sceening well for $U/W \lesssim 2$, but that once $U/W \sim 3$, electronic correlations reduce the screening by an order of magnitude [24]. This seems to be the problem with the LDA when applied to Ba$_2$Ca$_3$Cu$_4$O$_8$F$_2$, which is even nearly 2D. One might think of reducing all inter-layer hoppings as was recently done using the Gutzwiller approximation [25], but this would not directly change the metallic inter-layer screening, $1 + 2NM \sim 25$, where $2N \sim 0.6$ electrons/(eV·CuO$_2$) is the intra-layer density of states at the Fermi level and $M \sim 40$ eV·CuO$_2$/electron is the inter-layer Madelung constant. Instead, we perform selfconsistent LDA+U calculations for AF (π, π)-order and subsequently calculate band-structures and FSs for the charge potential, neglecting the spin potential. This procedure we denote $\langle$LDA+$U\rangle$. The result for the pure compound (q=0) is very similar to that obtained by the LDA and shown in the top right-hand quarter of Fig. 1. However, with an F-O exchange corresponding to q=0.02, we *do* obtain the proper splitting along the nodal line. This is shown in the bottom right-hand quarter of Fig. 1. The $\langle$LDA+$U\rangle$ procedure thus reduces the screening of this perturbation to about 2, but the pair-breaking argument why F-O exchange is an unlikely explanation for the anomalous ARPES FS remains valid. So from now on, we take q=0.

Next, we include the *calculated outwards dimple* of the *outer* O$_2$-layer (see Fig. 2), which is about the same in the LDA and the LDA+U. That this may induce a potential shift between the i- and o-layers can be seen as follows: For the calculated 0.07 Å $\sim \frac{1.54}{20}$ Å dimple, the bare value of the Cu^{2+}-(O^{2-})$_2$ dipole in the o-layer is $\frac{3\times 20\,\text{eV}}{20}$=3 eV, and after averaging over the Cu and O$_2$ sub-layers this yields a 2 eV bare Madelung shift of the o-layer with respect to the i-layer. Fig. 3 shows the $\langle$LDA+$U\rangle$ layer-averaged potential for all the Raman-active (even) dimples of the i and o-layers. We see that the intra-layer screening is substantial, that the inter-layer screening is about 4, and that for the calculated equilibrium structure, the $\langle$LDA+$U\rangle$ creates the proper 0.4 eV potential! The FS is very similar to the one calculated by adjusting the F-O exchange to reproduce the nodal splitting of the ARPES FS shown in the bottom right quarter of Fig. 1. Essentially the same FS is obtained by dimpling the i-layers outwards. In all cases, the n-sheets are on the i-layers and split by the hopping between them. The p-sheets are on the o-layers and almost degenerate; they agree less well with ARPES near the anti-nodal direction where the ARPES peaks are less well defined. Moreover, the ARPES data has been forced to yield the area, $1 \pm p$, proper for zero doping, which for the real material may not hold exactly. We have chosen to shift the Fermi level to fit ARPES along the nodal direction. In the bottom left-hand quarter of Fig. 1 we demonstrate that perfect agreement with ARPES can be obtained by adjustment of the vertical Ba and F positions.

If –in disagreement with the total-energy result– we dimple the o-layers or the i-layers *inwards* by 0.1 Å, the FS shown in the top left-hand quarter of Fig. 1 is obtained. Now the n-sheets are on the o-layers and unsplit, whereas the p-sheets are on the i-layers and split by the hopping between them.

There has recently been interest in possible consequences of poor z-axis screening for the electron-phonon interaction at small momentum transfers [26, 27]. We note that the coupling of the FS to an a_{1g} Raman-active dimpling mode via the screened Madelung-potential difference (once it exceeds the inter-layer hopping) is proportional to the Cu-O$_2$ distance, rather than to this distance squared, as is the case for the hopping-induced coupling considered earlier [28]. From Fig. 3 we realize that the deformation potential is sizeable: D=5 eV/Å. For a rough estimate of the associated electron-phonon coupling, let us like in Ref. [19] use the Hopfield expression, $\lambda = ND^2/\left(M\omega^2\right)$, to compare with MgB$_2$ for which λ≈1.0 : In Ba$_2$Ca$_3$Cu$_4$O$_8$F$_2$, the density of states appropriate for $d_{x^2-y^2}$-pairing is twice the value in MgB$_2$, D is 2.5 times smaller, and $M\omega^2$ is 1.3 times smaller for a Raman-active oxygen dimpling mode than for the optical bond-streching mode in MgB$_2$. Finally, the strong screening for large momentum transfers in Ba$_2$Ca$_3$Cu$_4$O$_8$F$_2$ effectively limits the integrand to the central half of the 2D Brillouin zone. As a result, $\lambda \sim \frac{1}{3}$, which suffices to enhance some other mechanism for HTSC.

We have shown *how* undoped Ba$_2$Ca$_3$Cu$_4$O$_8$F$_2$ manages to self-dope: By a dimpling distortion which is screened out poorly due to strong electronic correlations. This sets up an 0.4 eV difference in Madelung potential between the outer and inner layers, and that causes the FS to split along the nodal direction. The large Madelung-potential difference prevents interband scattering, and that seems to be the reason why two SC gaps survive. Since the dimpling is outwards according to our total-energy LAPW calculations, both in the LDA and in the LDA+U, the FS sheet with the small gap, the p-sheet, is located on the outer layers, next to the BaF-blocks where impurities are ubiquitous. This suggests that the p-gap is small because it is suppressed by impurity scattering, while the n-sheet is protected by the Madelung potential. The phase-diagram model, on the other hand, predicts the p-gap to be the largest. A further reason for the different gap sizes could be that, like in MgB$_2$ [18, 19], (one of) the interaction(s) driving the superconductivity is stronger for the n- than for the p-sheet. It could be of relevance that the bonding n-sheet has a larger effective intra-layer second-nearest neighbor Cu-Cu hopping integral, $t' + \frac{1}{8}t_\perp \sim 0.39t$, than the p-sheet, for which the effective value is merely $t' \sim 0.33t$, and therefore nests better along the [10]-directions. This would be consistent with the observation that for hole-doped multi-layer cuprates $T_{c\,\max}$ correlates positively with the largest sheet-value of t'/t [6].

Why these anomalies have been observed only in Ba$_2$Ca$_3$Cu$_4$O$_8$F$_2$ is undoubtedly due to the apical ions being F rather than O. Presumably, when going from apical O to the more ionic F, the covalency between Ba and the apical ion is reduced, whereby the covalency between Ba and O in the o-layer is strenghtened and causes it to dimple towards Ba. This is supported by the experimental finding that the outer layers in HgBa$_2$Ca$_4$Cu$_5$O$_{12+\delta}$ are dimpled inwards [29] or maybe flat [17, 30].

It will be interesting to follow the development of the Ba$_2$Ca$_3$Cu$_4$O$_8$(F$_{1-2p}$O$_{2p}$)$_2$ FS and its SC gaps as a function of hole-doping p. If our assignment of the p-sheets with the o-layers is correct, and as long as screening remains poor, O doping should suppress the gap on the p-sheet. Currently it is known that $T_{c\,\max}$=105 K is reached at p=0.20 [2], but no ARPES data are available.

We are grateful to O. Gunnarsson and J. Zaanen for useful discussions, to A. Yamasaki for checking calculations.

---

[1] Y. Chen *et al.,* preceding Letter.

[2] A. Iyo *et al.*, Physica C **392-396**, 140 (2003) and Supercond. Sci. Technol. **17**, 143 (2004).

[3] A. Damascelli *et al.*, Rev. Mod. Phys. **75**, 473 (2003).

[4] S. Chakravarty *et al.,* Science **261**, 337 (1993).

[5] O.K. Andersen *et al.*, J. Phys. Chem. Solids **56**, 1573 (1995).

[6] E. Pavarini *et al.,* Phys. Rev. Lett. **87**, 047003 (2001).

[7] Sahrakorpi *et al.* Phys. Rev. Lett. **95**, 157601 (2005).

[8] D.L. Feng *et al.*, Phys. Rev. Lett. **86**, 5550 (2001); Y.-D. Chuang *et al.*, Phys. Rev. Lett. **87**, 117002 (2001); A.A. Kordyuk *et al.*, Phys. Rev. B **66**, 014502 (2002).

[9] N.E. Hussey *et al.*, Nature **425**, 814 (2003).

[10] T.K. Kim *et al.,* Phys. Rev. Lett. **91,** 167002 (2003); A. Koitzsch *et al.*, Phys. Rev. B **69**, 140507(R) (2004).

[11] *Observed* mass-renormalizations are small and isotropic compared with those predicted by a one-band-per-layer Hubbard model with U=3.2 eV and LDA parameters, solved in the fluctuation-exchange approximation; A.I. Liechtenstein *et al.*, Phys. Rev. B **54**, 12505 (1996).

[12] A. G. Loeser *et al.*, Science **273**, 325 (1996).

[13] R. S. Markiewicz and A. Bansil, Phys. Rev. Lett. **96**, 107005 (2006).

[14] N. P. Armitage *et al.,* Phys. Rev. Lett. **88**, 257001 (2002).

[15] Y. Tokunaga *et al.,* Phys. Rev. B **61**, 9707 (2000); H. Kotegawa *et al.,* J. Phys. Chem. Solids **62**, 171 (2001).

[16] S. Chakravarty *et al.*, Nature **428**, 53 (2004); M. Mori and S. Maekawa, Phys. Rev. Lett. **94**, 137003 (2005)

[17] H. Kotegawa *et al.*, Phys. Rev. B **69**, 014501 (2004); H. Mukuda *et al.,* Phys. Rev. Lett. **96**, 087001 (2006).

[18] I. I. Mazin *et al,* Phys. Rev. Lett. **89,** 107002 (2002).

[19] L. Boeri *et al.,* Phys. Rev. Lett **93**, 237002 (2004).

[20] We used the WIEN2K implementation (K. Schwarz *et al.*, Comput. Phys. Commun. 147, 71 (2002)) of the LAPW method with the Ceperley-Alder LDA xc-potential as well as with the LDA+U scheme. $s_{\mathrm{Ca,Ba,Cu,O,F}}$=2.5, 2.6, 1.9, 1.7, 1.8 Bohr radii, $K_{\max}s_{\mathrm{O}}$=7.5, $l_{\max}$=10, and U_{dd}=5.4 eV.

[21] Going $\Delta k_{[110]}$ away from a FS sheet, the corresponding ARPES band first slopes ~3 times less and then, after a kink at ~0.07 eV, about the same as the LDA band.

[22] M.A. Beno *et al.*, Appl. Phys. Lett. **51**, 57 (1987).

[23] We used the 4-orbital model [5] and a formalism like G. Haran and A.D.S. Nagi, Phys. Rev. **54**, 15463 (1996).

[24] E. Koch *et al.*, Phys. Rev. Lett. **83**, 620 (1999).

[25] M. Mori *et al.*, J. Phys. Soc. Jpn. **75**, 034708 (2006).

[26] O. Rösch *et al.*, Phys. Rev. Lett. **95**, 227002 (2005).

[27] W. Meevasana *et al.*, Phys. Rev. Lett. **96**, 157003 (2006).

[28] D.J. Scalapino, Phys. Rep. **250**, 329 (1995); S.Y. Savrasov and O.K. Andersen, Phys. Rev. Lett. **77**, 4430 (1996); O.K. Andersen *et al.,* Journal of Low Temp. Phys. **105**, 285 (1996); O. Jepsen *et al.*, J. Phys. Chem. Solids **59**, 1718 (1998).

[29] J. Akimoto *et al.*, Physica C **281**, 237 (1997).

[30] Q. Huang *et al.*, Physica C **227**, 1 (1994).